Applied Geography 71 (2016) 106–114

Contents lists available at ScienceDirect

Applied Geography

journal homepage: www.elsevier.com/locate/apgeog

Combined vegetation volume and "greenness" affect urban air temperature

Amélie Y. Davis [a, b, *], Jinha Jung [b, c], Bryan C. Pijanowski [d], Emily S. Minor [b, e]

[a] Miami University, Department of Geography and Institute for the Environment and Sustainability, 234 Shideler Hall, Oxford, OH 45056, USA
[b] University of Illinois at Chicago, Institute for Environmental Science and Policy, 2121 West Taylor Street (MC 673), Chicago, IL 60612, USA
[c] Texas A&M University – Corpus Christi, 6300 Ocean Dr., Corpus Christi, TX 78414, USA
[d] Purdue University, Forestry and Natural Resources Department, 195 Marsteller St., West Lafayette, IN 47907, USA
[e] University of Illinois at Chicago, Biological Sciences, 845 W. Taylor Street (MC 066), Chicago IL 60607, USA

ARTICLE INFO

Article history:
Received 20 December 2015
Received in revised form
20 April 2016
Accepted 21 April 2016

Keywords:
LiDAR
NDVI
Urban heat island
Nighttime temperature
Cook County
3D

ABSTRACT

Cities are often substantially warmer than their surrounding rural areas. This 'urban heat island effect' can negatively affect the health of urban residents, increase energy usage, and alter ecological processes. While the effect of land use and land cover on urban heat islands has been extensively studied, little is known about the role of vegetation volume or built-area volume about this phenomenon. We ask whether the 3-dimensional structure of urban landscapes influences variations in temperature across a city. Using heights-above-ground information derived from LiDAR data and the Normalized Difference Vegetation Index (NDVI) calculated from multispectral (4 band: Blue, Green, Red, and Near Infrared) aerial images, we estimated vegetation volume and built-area volume (non-vegetated) in Chicago, Illinois (USA). Daily minimum temperature data were obtained from 36 weather stations for summer 2011. The differences in urban air temperature across the study area were as large as 3 °C. Maximum likelihood models indicated that a combination of NDVI and vegetation volume best predicted nighttime temperature in Chicago, and that vegetation growing within 250–500 m of the weather station was most influential. Our results indicate that vegetation in "the matrix", i.e. the area outside parks and preserves, is important in temperature mitigation since the majority of the vegetation volume in the study area occurs within residential, commercial/industrial, and institutional land uses. However, open space, which covers only 15% of the study area, has nearly as much total vegetation volume as residential land, which covers 61% of the study area. Clearly, both large wooded parks within a city and large trees scattered across residential areas are needed to best mitigate the urban heat island effect.

1. Introduction

Urban heat islands affect urban settlements worldwide. The degree to which the temperature in the city is augmented compared to its rural surroundings depends on regional context, such as the biome wherein the city is located and the city's size (Imhoff, Zhang, Wolfe, & Bounoua, 2010). Other factors, such as impervious surface extent, vegetation cover, and anthropogenic activities, are important too (Peng et al. 2012). In a study of 38 U.S. cities, yearly urban temperatures were on average 2.9 °C warmer than surrounding areas in all biomes except those with arid and semiarid climates (Imhoff et al. 2010). The effect is most pronounced on clear, still nights in the summer and has been detected both in surface and air temperatures (Voogt & Oke, 2003).

Urban heat islands can intensify summer heat waves, cause heat stress, and worsen air pollution (Loughner et al., 2012). Chicago, in particular, has suffered from heat waves, with the 1995 heat wave being responsible for over 700 deaths, mostly among low-income elderly individuals who did not have a strong social support system (Klinenberg, 2002). Other studies have shown that the most vulnerable members of society are also those most affected by extreme heat events (Buyantuyev & Wu, 2010; Harlan, Brazel, Prashad, Stefanov, & Larsen, 2006; Jenerette et al. 2007; Jenerette, Harlan, Stefanov, & Martin, 2011).

* Corresponding author. Miami University, Department of Geography and Institute for the Environment and Sustainability, 250 South Patterson Avenue, 213 Shideler Hall, Oxford, OH 45056, USA.
E-mail address: davis.amelie@miamiOH.edu (A.Y. Davis).

http://dx.doi.org/10.1016/j.apgeog.2016.04.010
0143-6228/

At the regional scale, it is well accepted that urban centers tend to be warmer than rural areas, especially in summer (U.S. EPA, 2015). More fine-scaled investigations, however, have found that land cover configuration and composition affect temperature, especially surface temperatures compared to air temperatures (Buyantuyev & Wu, 2010; Connors, Galletti, & Chow, 2013; Middel, Häb, Brazel, Martin, & Guhathakurta, 2014; Song, Du, Feng, & Guo, 2014; Myint, Wentz, Brazel, & Quattrochi, 2013). This effect depends partially on air flow through the urban area, which is a function of the spatial arrangement, size, and density of objects (buildings, trees, streets) in the city (Voogt & Oke, 2003). At the parcel scale, large deciduous trees planted on the eastern, southern, or western sides of homes decrease summer electricity use (Ko & Radke, 2013). One study (Ko & Radke, 2013), showed that the sum of tree height within 18.3 m of the western side of a property (as measured by LiDAR) decreased energy use the most, although occupant behavior most affected home energy consumption.

Mitigating urban heat island effects, especially in the face of climate change, is a goal for many municipalities (Akbari et al. 2008). Much research has focused on ascertaining the effect of vegetation cover or impervious surface cover on temperature in cities. Increased low albedo surfaces and impervious surfaces have been linked to elevated surface (Buyantuyev & Wu, 2010; Imhoff et al. 2010; Jenerette et al. 2007; Myint et al., 2013; Roth, Oke, & Emery, 1989; Weng, Lu, & Schubring, 2004; Yuan & Bauer, 2007) and air temperatures (Bowler, Buyung-Ali, Knight, & Pullin, 2010; Coseo & Larsen, 2014; Harlan et al. 2006) in urban areas.

Maps of vegetation cover or impervious surface area are usually derived from satellite imagery. Green space in particular is often estimated by calculating Normalized Difference Vegetation Index (NDVI) or Soil Adjusted Vegetation Index (SAVI). Since vegetation provides evaporative surfaces, heat storage capacity (Gallo et al. 1993) and shading, it can influence temperatures. Skelhorn et al. (2014) modeled surface and air temperature fluctuations in sub-urban areas of Manchester UK according to various greening scenarios. They found that a 5% increase in mature tree cover, versus hedges and young trees, decreased surface temperature by 1 °C and 0.5 °C respectively, while a 5% increase in grass cover increased surface temperature by 0.6 °C. No changes in air temperature were noted.

We estimated vegetation volume and built-area volume using LiDAR and multispectral (Red, Green, Blue, and Near Infrared bands) aerial images, and used weather station data from across Cook County, Illinois (USA), to determine whether built-area volume, vegetation volume (as a proxy for vegetation biomass), or NDVI is a stronger predictor of summer air temperature. Finally, we examined these relationships at 5 different scales (with buffers around the weather station ranging from 100 m to 1000 m) to determine the extent of any effects of our response variables on temperature.

2. Methods

2.1. Study area

In 2010, Cook County, Illinois (USA) had just over 5 million inhabitants (2010 U.S. Census). The county covers almost 2448 km^2 and borders Lake Michigan. Its climate is classified as humid continental, with four distinct seasons throughout the year. Cook County is home to Chicago, the third largest city in the United States in terms of population. In the Chicago region in 2010, there were an estimated 157 million trees that accounted for 15.5% of the total land cover, and 73.5% of these trees were less than 6 inches in diameter (Nowak et al. 2013).

2.2. Sample locations

Within Cook County, we located thirty-nine weather stations with nearly continuous data during our study period (Fig. 1). The three weather stations associated with the region's airports (O'Hare International Airport, Chicago Midway International Airport, and the Chicago Executive Airport) were removed from subsequent analyses because of the unusually large amount of impervious surface near the stations. Six weather stations were within 2 km of each other, so we randomly removed three of them from subsequent analyses to prevent overlap of the buffers. Our final data set comprises 33 weather stations, which serve as the center point for the ensuing landscape analyses. The mean (standard deviation), minimum, and maximum distance between nearest neighbor sites, i.e. nearest pairs of weather stations, are 4.9 (3.0), 2.1, and 13.5 km, respectively.

2.3. Temperature data

Minimum, maximum, and average daily temperatures for 2011 were downloaded from wunderground.com for the 33 Cook County weather stations. We used data from summer months (June 21 to September 21), as urban heat island effects are more pronounced in the summer (Imhoff et al. 2010; Myint et al. 2013; Yuan & Bauer, 2007). We used the daily minimum temperature as a proxy for nighttime temperature. We calculated an average of the daily minimum temperature over the three summer months. The mean daily minimum temperature at each weather station for summer 2011 was used as the response variable in our models, and is hereafter referred to as mean nighttime temperature.

We compared summer temperatures in 2011 to twenty year normal temperatures to summarily examine whether summer 2011 was a “typical summer” for our study region. The mean (low – high) normal (1981–2010) temperatures from O'Hare Airport's weather station (main airport situated at the North end of Cook County, Illinois) for June, July, August, and September are 20.5 (14.5–26.5), 23.3 (17.7–28.9), 22.4 (17.2–27.2), and 18.1 (12.4–23.8° Celsius), respectively (http://www.sws.uiuc.edu/atmos/statecli/General/chicago-climate-narrative.htm). Comparatively, the mean (low – high) temperature at the same weather station for June, July, August, and September 2011 were 21.1 (15.6–26.7), 26.1 (21.1–31.7), 23.3 (17.8–28.3), and 16.7 (12.2–20.6° Celsius; wunderground.com/history/airport/KORD), indicating that the summer of 2011 might have been slightly warmer than the average summer.

2.4. Estimation of vegetation volume, built-area volume, and NDVI

LiDAR data over Cook County were downloaded from the Illinois Height Modernization Program (ILHMP) web site. The LiDAR data acquisition occurred in November 2008 and April 2009. While that time of year is considered “leaf-off” in Cook County, LiDAR has been shown to reliably detect tree tops (maximum height) in leaf-off conditions, even for deciduous trees (Wasser, Day, Chasmer, & Taylor, 2013). The average density of the point cloud data was 5.05 point/m^2.

We adopted a 2D grid structure with 5 ft (1.5 m) spatial resolution for LiDAR data processing, so that each pixel had an average point density of 11.8 points/pixel. First, the point cloud data were classified into ground and non-ground points using LasTools (http://www.cs.unc.edu/~isenburg/lastools/). Then, a Digital Terrain Model (DTM) was generated by applying natural neighbor interpolation to ground points only. We chose a natural neighbor interpolation algorithm for DTM generation since it is

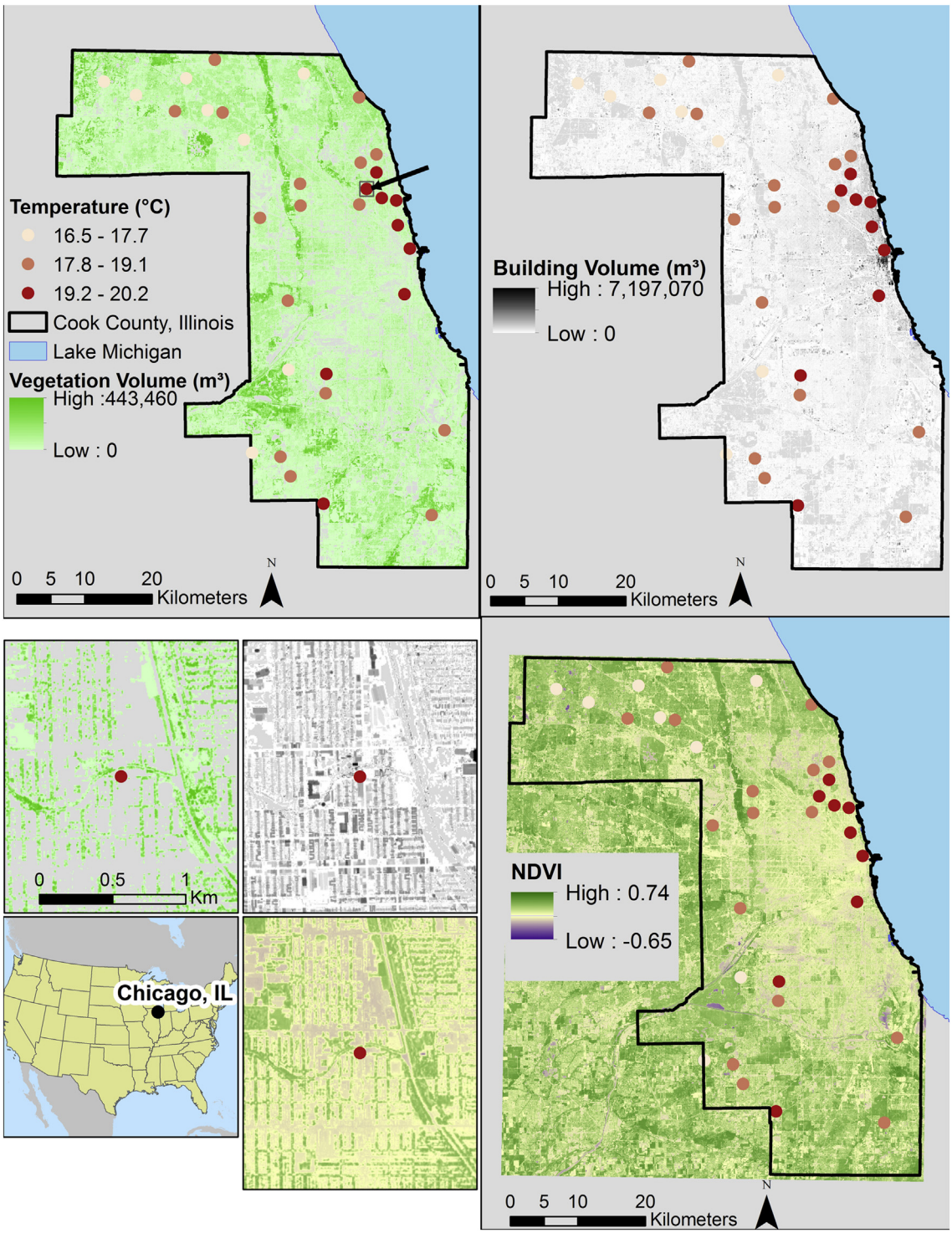

Fig. 1. Vegetation Volume (m^3), built-area volume (m^3), and NDVI are shown for Cook County, Illinois, USA, in the top left, top right, and bottom right panels, respectively. The points show the location of the weather stations used in this study and are color coded according to the mean temperature (°C) in the summer of 2011. In the top left panel, a box is drawn around one of the weather stations (indicated by an arrow). For that area, a close-up of each of the variables is shown in the bottom left panel, thus allowing for a comparison of the variables on a finer spatial scale. Negative NDVI represent water in the landscape. Aside from ponds (many of which are in Chicago's urban parks), a couple of rivers go through Cook County, Illinois. The inset on the bottom left corner shows the location of Cook County, Illinois within the conterminous USA.

known to generate reliable terrain models even in heavily vegetated environments (Kellner, Clark, & Hubbel, 2008). A Digital Surface Model (DSM) was generated by calculating maximum elevation of all points (both ground and non-ground) within each pixel. A Digital Height Model (DHM) was computed by subtracting the DTM from the DSM, so that the DHM represented height-above-ground and topographic effects were removed. Finally, the DHM was used to calculate volumetric estimates of objects on the ground by multiplying the height-above-ground value by area of the pixel.

Although LiDAR can provide volumetric information of objects on the ground, and structural characteristics of vegetation such as

forests (e.g., Jung & Pijanowski, 2012; Jung, Pekin, & Pijanowski, 2013; Mascaro, Detto, Asner, & Muller-Landau, 2011) it cannot differentiate between land covers. Normalized Difference Vegetation Index (NDVI) calculated from multispectral data is a well-known indicator (e.g. DeFries & Townshend 1994; Fensholt & Proud, 2012) that can be used to differentiate vegetation and non-vegetation classes. The NDVI map can be coupled with the volumetric estimates from the LiDAR data so that volume of vegetation and non-vegetation classes can be calculated separately. We used aerial orthomosaic images to generate an NDVI map of the study area. The aerial images were acquired in June 2010 as part of the USDA National Agriculture Image Program (NAIP). The NAIP images were delivered with a spatial resolution of 1 m and with 4 spectral bands; red (R), green (G), blue (B), and near infrared (NIR). The NDVI layer of Cook County at 1 m spatial resolution was generated using Eq. (1).

$$\mathrm{NDVI} = (\mathrm{NIR} - \mathrm{R})/(\mathrm{NIR} + \mathrm{R}) \quad (1)$$

We performed a binary classification (vegetation vs. non-vegetation class) using 0.2 as an NDVI threshold value. The threshold value was selected based on suggested values in previous studies (Xu, 2007) and after visually inspecting the binary classification map by overlaying the fine spatial resolution aerial images. The binary classification results were used to calculate volumetric estimates of vegetation and non-vegetation classes. The non-vegetation volume is hereafter referred to as built-area volume. Vegetation volume and built-area volume were measured in km^3 and calculated as the total value within various buffers around the weather station.

We created a 3D vegetation index by multiplying normalized vegetation volume (calculated by dividing the sum of vegetation volume in each buffer by the maximum value of the sum of vegetation volume in the buffers across the study area) by NDVI. Together these represent both a measure of the volume of the vegetation and its "greenness", i.e. a 3D NDVI. We assumed that areas with high values of 3D NDVI have denser stands of trees. Vegetation volume, built-area volume, NDVI, and 3D NDVI were all measured at multiple buffer distances around each weather station (100, 250, 500, 750 and 1000 m). We also measured distance from each weather station to Lake Michigan. Table 1 provides the summary statistics for these variables. We expected that, in summer, nighttime temperature would increase as built-area volume increased and would decrease as vegetation volume, NDVI, and 3D NDVI increased.

2.5. Modeling

We aimed to test the importance of vegetation volume as an explanatory factor in nighttime air temperature and to characterize the response of nighttime temperature to variations in vegetation volume, built-area volume, and NDVI. Elevation and distance to Lake Michigan were hypothesized to affect temperature as well, yet they were strongly correlated (rho = 0.85, $p < 0.001$, n = 33, Table A1). Thus, only distance to Lake Michigan was retained in subsequent models. We checked for multicollinearity in our explanatory variables at each scale of analysis by calculating Variance Inflation Factors (VIFs) using the R (R Core Team, 2013) package *usdm*. We log-transformed built-area volume to improve linear relationships. Four linear regression models were examined:

(1) temperature = a + b(distance to lake) + c(vegetation volume) + ε
(2) temperature = a + b(distance to lake) + c(log(built-area volume)) + ε
(3) temperature = a + b(distance to lake) + c(NDVI) + ε
(4) temperature = a + b(distance to lake) + c(3D NDVI) + ε

The maximum likelihood estimates of the model parameters (a, b, c) were estimated using simulated annealing, a global optimization algorithm (Goffe, Ferrier, & Rogers, 1994). This was completed in R using the *likelihood* package (Murphy, 2012). We used default settings, a normal probability density function, 10,000 iterations, and all initial lower and upper bounds for the parameters were set at −100,000, and 100,000 respectively. Model selection was completed using AICc in R (version 3.0.1), with the best models having high R^2 and lower ΔAICc. Residuals of all the models were visually examined for heteroscedasticity, outliers, and other patterns. None were detected.

2.6. Assessing volume and greenness metrics across land use types

We used Land Use Inventory data from 2010, provided by Chicago Metropolitan Agency for Planning (available here http://www.cmap.illinois.gov/data/land-use/inventory), to assess the allocation of land, vegetation volume, mean NDVI, and mean 3D NDVI in the various land use types found across the study area. The various land use types from the Land Use Inventory are "Agriculture" (land use code of 2000); "Vacant" which includes undeveloped land and land under construction (land use code 4000); "Developed" (land use code 1000) which combines residential, industrial, commercial, institutional, and transportation; "Open Space" (land use code 3000) which includes forest preserves, golf courses, public and private open space, and trails; and "Other" which includes so called 'non parcel areas' (land use code 6000) such as road rights-of-way. Water parcels and parcels that are labelled as not classifiable (land use codes of 5000, and 9999, respectively) were removed from subsequent analyses. They represented 0.33 and 0.05% of the land use in Cook County, respectively.

2.7. Potential limitations of approach

We were limited by the availability of datasets. LiDAR data and high spatial resolution aerial images for our study area were only freely available at the times specified above. Since the datasets are within three years of each other, collected during a severe economic recession, and Cook County is already highly developed, it is unlikely that the green and grey infrastructure within the area changed substantially over that time period. Lastly, it is important that NDVI be at or near its peak for the results to be tenable. Given that Cook County is situated in the Northern Hemisphere at mid-latitudes, the month of June is considered late Spring, early summer, which would coincide with near peak NDVI values.

3. Results

Models explained between 44% and 63% of the spatial variation in mean nighttime temperature. The best model (based on AICc and R^2) included NDVI and vegetation volume as predictor variables (Table 2). Built-area volume explained the least amount of variation and most models that included this predictor variable had the highest AICc. Vegetation volume, NDVI, and 3D NDVI had negative relationships with temperature, while built-area volume had a positive relationship with temperature (Table 2, c parameter). In all models, the b parameter was negative, meaning that nighttime temperature was lower for stations that were further away from Lake Michigan (Table 2 and Fig. 1). All of the VIFs were less than 4 (Table B1) indicating that our models were properly specified.

The best scale of analysis depended on the predictor variable. Of several models tested, 3D NDVI had the most explanatory power when measured in 500 m buffers around the weather stations

Table 1
Summary statistics for variables used in the models (n = 33 weather stations).

Variable	Mean (SD)	Minimum	Maximum
Elevation (m)	200.29 (23.15)	176.46	269.89
Distance to lake (km)	15.21 (10.78)	0.76	35.02
Sum of vegetation volume within 100 m (km^3)	0.03 (0.02)	0.00	0.08
Sum of vegetation volume within 250 m (km^3)	0.17 (0.11)	0.01	0.46
Sum of vegetation volume within 500 m (km^3)	0.72 (0.4)	0.10	1.49
Sum of vegetation volume within 750 m (km^3)	1.68 (0.9)	0.24	3.38
Sum of vegetation volume within 1000 m (km^3)	3.04 (1.62)	0.50	6.88
Sum of built-area volume within 100 m (km^3)	0.03 (0.03)	0.00	0.18
Sum of built-area volume within 250 m (km^3)	0.15 (0.17)	0.00	0.87
Sum of built-area volume within 500 m (km^3)	0.65 (0.84)	0.01	4.71
Sum of built-area volume within 750 m (km^3)	1.48 (2.05)	0.04	11.78
Sum of built-area volume within 1000 m (km^3)	2.63 (3.74)	0.41	21.47
Mean of NDVI within 100 m	0.16 (0.11)	−0.05	0.35
Mean of NDVI within 250 m	0.17 (0.1)	−0.06	0.32
Mean of NDVI within 500 m	0.18 (0.09)	0.01	0.34
Mean of NDVI within 750 m	0.18 (0.09)	0.02	0.31
Mean of NDVI within 1000 m	0.19 (0.09)	0.03	0.30

Table 2
Comparison of model outputs.

Model	AICc	R^2	ΔAICc	a	b	c
Vegetation volume - 100 m	84.8	0.48	11.1	19.97	−0.07	−16.81
Vegetation volume - 250 m	81.23	0.54	7.53	20.12	−0.06	−3.82
Vegetation volume - 500 m	77.03	0.59	3.33	20.27	−0.06	−1.2
Vegetation volume - 750 m	78.91	0.57	5.21	20.28	−0.06	−0.53
Vegetation volume - 1 km	78.75	0.57	5.05	20.27	−0.05	−0.31
Built-area volume - 100 m	79.26	0.56	5.56	21.26	−0.04	0.53
Built-area volume - 250 m	85.68	0.47	11.98	20.1	−0.05	0.37
Built-area volume - 500 m	86.41	0.46	12.71	19.48	−0.04	0.32
Built-area volume - 750 m	84.32	0.49	10.62	19.06	−0.03	0.5
Built-area volume - 1 km	80.35	0.55	6.65	18.44	−0.02	0.72
NDVI - 100 m	85.09	0.48	11.39	19.82	−0.05	−3.51
NDVI - 250 m	81.6	0.53	7.9	19.96	−0.04	−4.83
NDVI - 500 m	80.3	0.55	6.6	20.07	−0.04	−5.31
NDVI - 750 m	77.93	0.58	4.23	20.23	−0.03	−6.6
NDVI - 1 km	76.56	0.6	2.86	20.29	−0.03	−6.85
3D NDVI - 100 m	80.73	0.54	7.03	19.8	−0.06	−5.69
3D NDVI - 250 m	74.57	0.62	0.87	19.95	−0.06	−7.16
3D NDVI - 500 m	73.7	0.63	0	19.94	−0.06	−5.87
3D NDVI - 750 m	76.17	0.6	2.47	19.89	−0.05	−5.75
3D NDVI - 1 km	76.9	0.59	3.2	19.87	−0.05	−6.45

($R^2 = 0.63$, Figs. 2 and 3), but the 250 m resolution was also a good model with ΔAICc less than 2 (Table 2). On the other hand, the explanatory power of built-area volume was greatest at the smallest buffer size ($R^2 = 0.56$ at the 100 m scale) and was smallest at intermediate buffer sizes (Fig. 2). NDVI explained the most variation at the largest buffer ($R^2 = 0.60$) and the least variation when measured in 100 m buffers ($R^2 = 0.48$, Fig. 2). When considered alone, vegetation volume best explained the variation in temperature when measured in the 500 m radius ($R^2 = 0.59$) but the 750 m model cannot be differentiated statistically (Table 2).

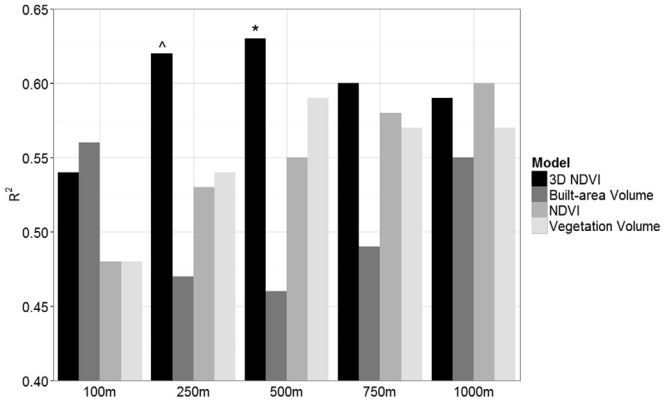

Fig. 2. R^2 values for the four different models at the 5 spatial scales. The model with the lowest AIC is designated by an asterisk (*) above its column. The one competing model (within 2 ΔAIC of the best model) is designated by a carrot (^).

In general, mean nighttime temperature for summer 2011 varied by 3 °C across the city, whereas higher temperatures were observed in areas with less vegetation volume and lower NDVI (Fig. 3 for the 500 m scale; other scales showed similar patterns although the relationship between sum of vegetation volume and mean NDVI at the 100 m scale was the weakest).

The Land Use Inventory data revealed interesting trends in vegetation patterns across the city (Fig. 4). Developed land (residential, industrial, commercial, institutional, and transportation) accounted for the majority of the area (61%), and also contained the greatest total vegetation volume in the city. Open space (forest preserves, golf courses, public and private open space, and trails) only accounted for 15% of the study area but these areas contained the second highest total vegetation volume and had the highest mean 3D NDVI values of all land uses. The "other" category, which consists mostly of road rights-of-way, accounted for 17% of the land, and had the second largest mean 3D NDVI value.

4. Discussion

Our models were able to explain 63% of the spatial variation in urban air temperature based on NDVI and vegetation volume measured in a 500 m buffer around weather stations. While NDVI and vegetation volume alone each explain a fair amount of variation in temperature, they performed best when considered together. NDVI is a good measure of vegetative vigor (i.e. plant health and photosynthetic activity), as high values of NDVI indicate actively growing plants with many chlorophyll cells and mesophyll tissue (Campbell, 2002). Vegetation that is stressed due to heat, lack of water, or disease will have a lower NDVI than the same volume of healthy vegetation. Similarly, older trees, which are less photosynthetically active than young trees (Ryan, Binkley, & Fownes, 1997), would have lower NDVI than similarly-sized young trees. NDVI is also known to be influenced by leaf area index, canopy shape and cover, species composition, land cover type, leaf optics, understory vegetation, and biomass (Huete et al. 2002). On the other hand, vegetation volume (as

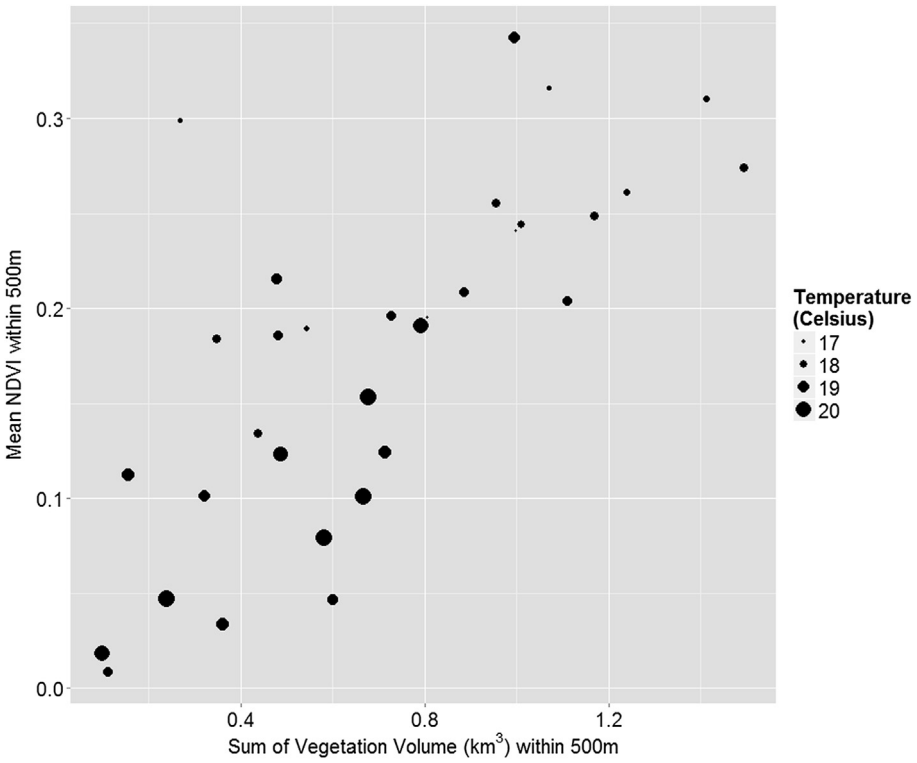

Fig. 3. Relationship between mean NDVI within 500 m of the weather station, sum of Vegetation Volume within 500 m of the weather station, and mean nighttime air temperature at the weather station between June 21 and September 21 2011.

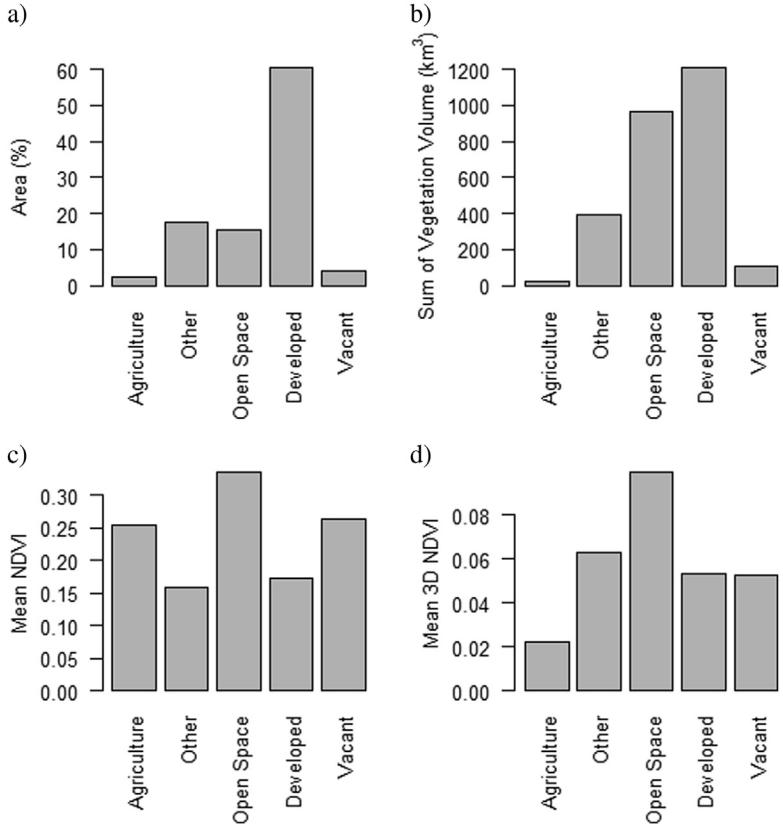

Fig. 4. a) Percent of study area in the various land uses in Cook County IL. b) Sum of vegetation volume by land use. c) Mean NDVI by land use. d) Mean 3D NDVI by land use. The various land use types are “Agriculture”; “Vacant” which includes undeveloped land and land under construction; “Developed” which combines residential, industrial, commercial, institutional, and transportation; “Open Space” which includes forest preserves, golf courses, public and private open space, and trails; and “Other” which includes so called ‘non parcel areas’ such as right-of-ways.

measured by LiDAR) indicates the total amount of vegetation, whether it is growing vigorously or not. Vegetation volume is most likely distinguishing grass from trees, which would help explain temperature differences since trees have a higher transpiration rate than grasses and thus provide more cooling. Indeed, increased vegetation volume helped reduce the urban heat island effect in Amsterdam (Rafiee, Dias, & Koomen, 2016). However, areas of low vegetation volume, such as turf grass, also modify urban temperature, with some studies modeling an increase in surface temperature with increased turf grass cover (Skelhorn et al. 2014 for Manchester UK) and others observing a decrease (Myint et al. 2013 for Phoenix AZ). We think vegetation volume and NDVI provide complementary information, which might explain why the combination of NDVI and vegetation volume (what we refer to as 3D NDVI) is a better predictor of urban air temperature in Cook County, Illinois, than either variable alone.

Most interestingly, it seems that the effect of combined vegetation cover and volume is strongest at intermediate spatial resolutions (500 m from the weather station), and that the sphere of influence of 3D NDVI on temperature is smaller than that of NDVI alone. In a study conducted in Indianapolis IN, Weng et al. (2004) found that the strongest (negative) correlation between NDVI and surface temperature occurred at a scale of 120 m. In Beijing, China, Song et al. (2014) found that the relationship between surface temperature and land cover was strongest at 660 and 720 m scales. These results are in line with ours and the differences in the importance of scales may be due to differences in physical characteristics of the cities themselves (block size, building density, percent grey and green infrastructure, etc.), study design (none of the temperature sensors in our study were located in forest preserves or Chicago's large urban parks), and of course regional climate characteristics.

From an urban planning standpoint, the implication of these results is that a city needs to not just spread out green space, but also spread out mature trees, or at the very least nurture existing mature trees. The major implication of these findings is that neighborhoods with mature trees are reaping substantially more benefits in terms of microclimate or urban heat island reduction than neighborhoods that “just” have young trees, smaller trees, and grassy parks. Indeed, we see a 3 °C range in temperature across our study area.

The medium-large buffer size in the best model indicates that broad vegetation cover has a greater influence on mitigating temperatures compared to vegetation at more local scales. Practically, this might imply that spreading any vegetation (shrubs, and young and old trees) throughout a city could be a good approach to mitigating urban heat island effects, i.e. a land sharing approach rather than land sparing. This approach has also been suggested by Rotem-Mindali, Michael, Helman, and Lensky (2015) after an analysis of local land use on the urban heat island effect in Tel Aviv. On the other hand, it is well known that vegetated parks act as “cool islands” (Chang et al., 2007; Feyisa et al., 2014; Yu & Hien, 2006) and other research has shown that as park size increases, urban air temperature near the park decreases (Cao, Onishi, Chen, & Imura, 2010). Our study illustrates the importance of the matrix, i.e. non-park vegetation, for temperature mitigation since the majority of the vegetation volume in the study area occurs within residential, commercial/industrial, and institutional land uses. However, open space has nearly as much total vegetation volume as the developed land use category yet only accounts for approximately 15% of the study area, while developed land use accounts for nearly 61% of the study area. Clearly, a combination of having both large wooded parks within a city and large trees scattered across developed areas are necessary, especially when multiple ecosystem services are considered beyond temperature mitigation (Stott, Soga, Inger, & Gaston, 2015).

In contrast to vegetation, the effect of built-area volume (not accounting for different building materials) was local; this variable had the most explanatory power when measured within 100 m of the weather stations. Using built-area volume standards to mitigate urban heat island effects would be impractical, given that spreading buildings out would be detrimental from a land-use and housing-density perspective, as well as other related urban planning issues.

We also note that temperatures at weather stations near Lake Michigan are warmer than more inland stations. The coast, with its proximity to beaches and trails along it, is a desirable location to live in the city, which means that there are strong pressures to provide housing and other grey infrastructure near it, at the expense of green infrastructure. Indeed, areas closest to downtown Chicago are associated with high building volume, low vegetation volume, and low NDVI. Additionally, the lake provides cooling nearby during warm days, when air over the city heats up, rises, and is replaced by cooler air from over the lake, but we hypothesize that this lake breeze effect is not present at night or might even reverse itself.

4.1. Future research

This research should be repeated in other cities with varying climates and of varying sizes to determine whether the relationship holds in those localities, and to see if a simple equation could help characterize the relationship between vegetation volume, NDVI, and urban air temperature across multiple cities. Future research might also include comparing the index we propose here to leaf area index or plant biomass measures, and relating those to air temperatures across an urban to rural gradient, rather than just within an urban area.

5. Conclusion

The uniqueness of our study lies in our 3-dimensional vegetation component and the fact that we examined air temperature rather than surface temperature. We also used multiple months of data, conducted this research in a humid continental climate (many studies were undertaken in a semi-arid climate by the Phoenix LTER, where trees are less common), and our weather stations span an urbanization gradient, i.e. from downtown Chicago to less dense suburban areas. We found that a combination of vegetation volume and NDVI best explained differences in urban air temperature which, in summer 2011, were observed to be as large as 3 °C across Cook County, Illinois. These findings may have implications for many cities in the Midwest, which have recently taken management actions to deal with the emerald ash borer invasion. Many of them have decided to remove all ash trees within their jurisdiction, yet this research provides more support that investing in treatment options would be highly beneficial, even for older trees, given the temperature mitigation and other ecosystem services they are known to provide.

Acknowledgements

This research was supported by the U.S. Forest Service and the National Science Foundation under the ULTRA-Ex program (grant number 0948484). The authors wish to thank Jamie Brocker for finding and summarizing some of the research articles used in the introduction, as well as Dr. Charles Canham for teaching us some of the methods used in this paper at the “Likelihood Methods in Ecology” workshop in 2013.

Appendix A

Table A1
Pearson correlations between variables (p-values are not adjusted for multiple comparisons). VV stands for Vegetation Volume, BV stands for Built-area Volume, and NDVI stands for Normalized Difference Vegetation Index.

	Dist. to lake	Elevatici	Sum of vegetation volume (100m)	Mean of NDVI (100m)	Sum of built-are volume (100m)	Sum of Vegetatio Volume (250m)	Mean of NDVI (250m)	Sum of built-are volume (250m)	Sum of vegetation volume (500m)	Mean of NDVI (500m)	Sum of built-are volume (500m)	Sum of vegetatio volume (750m)	Mean of NDVI (750m)	Sum of built-are a volume (750m)	Sum of vegetation volume (lkm)	Mean of NDVI (lkm)	Sum of built-area volume (1km)
Temperature	−0.61 ***	−0.67 ***	−0.25	−0.56 ***	0.62 ***	−0.36 *	−0.62 ***	0.62***	−0.48 **	−0.64***	0.56***	−0.51 **	−0.7***	0.54**	−0.53**	−0.73***	0.54**
Dist. to lake		0.81 ***	−0.14	0.42*	−0.51 **	−0.07	0.43*	−0.58 ***	0.01	0.41*	−0.53**	0.11	0.49 **	−0.51 **	0.14	0.53**	−0.51**
Elevation			−0.03	0.26	−0.38 *	0.02	0.32	−0.43 *	0.16	0.33	−0.39 *	0.24	0.43 *	−0.37 *	0.23	0.47**	−0.37*
Sum of VV (100m)				0.54**	−0.28	0.91***	0.51 **	−0.29	0.74 ***	0.49 **	−0.24	0.61***	0.46 **	−0.24	0.53 **	0.44**	−0.24
Mean NDVI (100m)					−0.52 **	0.66***	0.93 ***	−0.6***	0.62 ***	0.88 ***	−0.51**	0.52 **	0.84 ***	−0.47 **	0.46**	0.82***	−0.46**
Sum BV (100m)						−0.35 *	−0.57 ***	0.98***	−0.41 *	−0.62***	0.98 ***	−0.44*	−0.64***	0.97 ***	−0.44*	−0.66***	0.97***
Sum of VV (250m)							0.66 ***	−0.38 *	0.89 ***	0.65***	−0.33	0.74***	0.61 ***	−0.33	0.65 ***	0.58 ***	−0.32
Mean NDVI (250m)								−0.65 ***	0.7***	0.96 ***	−0.57 ***	0.63 ***	0.93 ***	−0.53 **	0.57 ***	0.91***	−0.52 **
Sum of BV (250m)									−0.44 *	−0.63 ***	0.98 ***	−0.44 **	−0.71 ***	0.96 ***	−0.44*	−0.72***	0.96 ***
Sum of VV (250m)										0.74 ***	−0.4*	0.95 ***	0.73 ***	−0.4*	0.86 ***	0.72 ***	−0.38*
Mean NDVI (500m)											−0.61***	0.68***	0.98 ***	−0.58 ***	0.62***	0.95 ***	−0.56***
Sum of BV (500m)												−0.42 *	−0.64***	1***	−0.42*	−0.65***	0.99 ***
Sum of VV (750m)													0.72 ***	−0.42 *	0.96***	0.73 ***	−0.42*
Mean NDVI (750m)														−0.61 ***	0.68 ***	0.99 ***	−0.6 ***
Sum of BV (750m)															−0.43 *	−0.63 ***	1***
Sum of VV (1km)																0.71 ***	−0.42 *
Mean NDVI (1km)																	−0.62***

Appendix B

Table B1
Variance Inflation Factors (VIFs) for variables included in models at the different scales of analysis. VIFs are only to be compared within columns.

	100 m	250 m	500 m	750 m	1000 m
Dist. to lake	1.91	2.15	1.83	1.76	1.8
Vegetation volume	1.89	2.53	2.84	2.56	2.37
NDVI	2.2	3.23	3.59	3.52	3.47
Built-area volume	1.68	2.25	1.92	1.78	1.76

References

Akbari, H., Bell, R., Brazel, T., Cole, D., Estes, M., Heisler, G., et al. (2008). Reducing urban heat islands: compendium of strategies. *Environmental Protection Agency*. retrieved July, 12, 2015 https://www.epa.gov/sites/production/files/2014-06/documents/basicscompendium.pdf.

Bowler, D. E., Buyung-Ali, L., Knight, T. M., & Pullin, A. S. (2010). Urban greening to cool towns and cities: a systematic review of the empirical evidence. *Landscape and Urban Planning, 97*(3), 147–155.

Buyantuyev, A., & Wu, J. (2010). Urban heat islands and landscape heterogeneity: linking spatiotemporal variations in surface temperatures to land-cover and socioeconomic patterns. *Landscape Ecology, 25*(1), 17–33.

Campbell, J. B. (2002). *Introduction to remote sensing*. CRC Press.

Cao, X., Onishi, A., Chen, J., & Imura, H. (2010). Quantifying the cool island intensity of urban parks using ASTER and IKONOS data. *Landscape and Urban Planning, 96*(4), 224–231.

Chang, C. R., Li, M. H., & Chang, S. D. (2007). A preliminary study on the local cool-island intensity of Taipei city parks. *Landscape and Urban Planning, 80*(4), 386–395.

Connors, J. P., Galletti, C. S., & Chow, W. T. (2013). Landscape configuration and urban heat island effects: assessing the relationship between landscape characteristics and land surface temperature in Phoenix, Arizona. *Landscape Ecology, 28*(2), 271–283.

Coseo, P., & Larsen, L. (2014). How factors of land use/land cover, building configuration, and adjacent heat sources and sinks explain Urban Heat Islands in Chicago. *Landscape and Urban Planning, 125*, 117–129.

DeFries, R. S., & Townshend, J. R. G. (1994). NDVI-derived land cover classifications at a global scale. *International Journal of Remote Sensing, 15*(17), 3567–3586.

Fensholt, R., & Proud, S. R. (2012). Evaluation of earth observation based global long term vegetation trends—Comparing GIMMS and MODIS global NDVI time series. *Remote Sensing of Environment, 119*, 131–147.

Feyisa, G. L., Dons, K., & Meilby, H. (2014). Efficiency of parks in mitigating urban heat island effect: an example from Addis Ababa. *Landscape and Urban Planning, 123*, 87–95.

Gallo, K. P., McNab, A. L., Karl, T. R., Brown, J. F., Hood, J. J., & Tarpley, J. D. (1993). The use of a vegetation index for assessment of the urban heat island effect. *International Journal of Remote Sensing, 14*(11), 2223–2230.

Goffe, W. L., Ferrier, G. D., & Rogers, J. (1994). Global optimization of statistical functions with simulated annealing. *Journal of Econometrics, 60*(1), 65–99.

Harlan, S. L., Brazel, A. J., Prashad, L., Stefanov, W. L., & Larsen, L. (2006). Neighborhood microclimates and vulnerability to heat stress. *Social Science & Medicine, 63*(11), 2847–2863.

Huete, A., Didan, K., Miura, T., Rodriguez, E. P., Gao, X., & Ferreira, L. G. (2002). Overview of the radiometric and biophysical performance of the MODIS vegetation indices. *Remote Sensing of Environment, 83*(1), 195–213.

Imhoff, M. L., Zhang, P., Wolfe, R. E., & Bounoua, L. (2010). Remote sensing of the urban heat island effect across biomes in the continental USA. *Remote Sensing of Environment, 114*(3), 504–513.

Jenerette, G. D., Harlan, S. L., Brazel, A., Jones, N., Larsen, L., & Stefanov, W. L. (2007). Regional relationships between surface temperature, vegetation, and human settlement in a rapidly urbanizing ecosystem. *Landscape Ecology, 22*(3), 353–365.

Jenerette, G. D., Harlan, S. L., Stefanov, W. L., & Martin, C. A. (2011). Ecosystem services and urban heat riskscape moderation: water, green spaces, and social inequality in Phoenix, USA. *Ecological Applications, 21*(7), 2637–2651.

Jung, J., Pekin, B. K., & Pijanowski, B. C. (2013). Mapping open space in an old-growth, secondary-growth, and selectively-logged tropical rainforest using discrete return LIDAR. Selected Topics in Applied Earth Observations and Remote Sensing. *Institute of Electrical and Electronics Engineers Journal of Selected Topics in Applied Earth Observations and Remote Sensing, 6*(6), 2453–2461.

Jung, J., & Pijanowski, B. (2012). Mapping vegetation volume in urban environments by fusing LiDAR and multispectral data. *Korean Journal of Remote Sensing, 28*(6).

Kellner, J. R., Clark, D. B., & Hubbel, S. P. (2008). Pervasive canopy dynamics produce short-term stability in a tropical rain forest landscape. *Ecology Letters, 12*(2), 155–164.

Klinenberg, E. (2002). *Heat wave: A social autopsy of disaster in chicago*. University of Chicago Press.

Ko, Y., & Radke, J. (2013). The effect of urban form and residential cooling energy use in Sacramento, California. *Environment and planning B: Planning and Design, 40*.

Loughner, C. P., Allen, D. J., Zhang, D. L., Pickering, K. E., Dickerson, R. R., & Landry, L. (2012). Roles of urban tree canopy and buildings in urban heat island effects: parameterization and preliminary results. *Journal of Applied Meteorology and Climatology, 51*(10), 1775–1793.

Mascaro, J., Detto, M., Asner, G. P., & Muller-Landau, H. C. (2011). Evaluating uncertainty in mapping forest carbon with airborne LiDAR. *Remote Sensing of Environment, 115*(12), 3770–3774.

Middel, A., Häb, K., Brazel, A. J., Martin, C. A., & Guhathakurta, S. (2014). Impact of urban form and design on mid-afternoon microclimate in Phoenix Local Climate Zones. *Landscape and Urban Planning, 122*, 16–28.

Murphy, L. (2012). *Likelihood: Methods for maximum likelihood estimation. R package version 1.5*. http://CRAN.R-project.org/package=likelihood.

Myint, S. W., Wentz, E. A., Brazel, A. J., & Quattrochi, D. A. (2013). The impact of distinct anthropogenic and vegetation features on urban warming. *Landscape Ecology, 28*(5), 959–978.

Nowak, D. J., Hoehn, R. E., III, Bodine, A. R., Crane, D. E., Dwyer, J. F., Bonnewell, V., et al. (2013). *Urban trees and forests of the chicago region*. Newton Square, Pennsylvania, US: Resource Bulletin NRS-84 of the US Forest Service Northern Research Station.

Peng, S., Piao, S., Ciais, P., Friedlingstein, P., Ottle, C., Breon, F. M., … Myneni, R. B. (2012). Surface urban heat island across 419 global big cities. *Environmental Science & Technology, 46*(2), 696–703.

R Core Team. (2013). *R: A language and environment for statistical computing*. Vienna, Austria: R Foundation for Statistical Computing. URL http://www.R-project.org/.

Rafiee, A., Dias, E., & Koomen, E. (2016). Local impact of tree volume on nocturnal urban heat island: a case study in Amsterdam. *Urban Forestry & Urban Greening, 16*, 50–61.

Rotem-Mindali, O., Michael, Y., Helman, D., & Lensky, I. M. (2015). The role of local land-use on the urban heat island effect of Tel Aviv as assessed from satellite remote sensing. *Applied Geography, 56*, 145–153.

Roth, M., Oke, T. R., & Emery, W. J. (1989). Satellite-derived urban heat islands from three coastal cities and the utilization of such data in urban climatology. *International Journal of Remote Sensing, 10*(11), 1699–1720.

Ryan, M. G., Binkley, D., & Fownes, J. H. (1997). Age-related decline in forest productivity. *Adv. Ecol. Res., 27*, 213–262.

Skelhorn, C., Lindley, S., & Levermore, G. (2014). The impact of vegetation types on air and surface temperatures in a temperate city: a fine scale assessment in Manchester UK. *Landscape and Urban Planning, 121*, 129–140.

Song, J., Du, S., Feng, X., & Guo, L. (2014). The relationships between landscape compositions and land surface temperature: quantifying their resolution sensitivity with spatial regression models. *Landscape and Urban Planning, 123*, 145–157.

Stott, I., Soga, M., Inger, R., & Gaston, K. J. (2015). Land sparing is crucial for urban ecosystem services. *Frontiers in Ecology and the Environment, 13*(7), 387–393.

U.S. Environmental Protection Agency. (December 4, 2015). Heat island effect. Retrieved from http://www.epa.gov/heat-islands.

Voogt, J. A., & Oke, T. R. (2003). Thermal remote sensing of urban climates. *Remote Sensing of Environment, 86*(3), 370–384.

Wasser, L., Day, R., Chasmer, L., & Taylor, A. (2013). Influence of vegetation structure on lidar-derived canopy height and fractional cover in forested riparian buffers during leaf-off and leaf-on conditions. *PloS one, 8*(1), e54776.

Weng, Q., Lu, D., & Schubring, J. (2004). Estimation of land surface temperature–vegetation abundance relationship for urban heat island studies. *Remote sensing of Environment, 89*(4), 467–483.

Xu, H. (2007). Extraction of urban built-up land features from Landsat imagery using a thematic oriented index combination technique. *Photogrammetric Engineering & Remote Sensing, 73*(12), 1381–1391.

Yuan, F., & Bauer, M. E. (2007). Comparison of impervious surface area and normalized difference vegetation index as indicators of surface urban heat island effects in Landsat imagery. *Remote Sensing of Environment, 106*(3), 375–386.

Yu, C., & Hien, W. N. (2006). Thermal benefits of city parks. *Energy and Buildings, 38*(2), 105–120.